PHYSICAL REVIEW B **69**, 205407 (2004)

Modeling of stick-slip phenomena using molecular dynamics

D. Mulliah, S. D. Kenny, and Roger Smith
Modeling of Materials Group, Department of Mathematical Sciences, Loughborough University, Loughborough, Leicestershire LE11 3TU, United Kingdom

(Received 23 January 2004; revised manuscript received 15 March 2004; published 21 May 2004)

Molecular dynamics simulations are performed to investigate the atomic-scale stick-slip phenomenon of a pyramidal diamond tip inserted into the Ag(010) surface. The mechanisms behind the stick-slip events are investigated by considering sliding speeds between 1.0 and 5.0 ms^{-1} and vertical support displacements of 5 and 15 Å. The analysis of the dynamic features of the substrate shows that dislocations are extrinsically linked to the stick events, with the emission of a dislocation in the substrate region near the tip, when slip occurs after stick. For small vertical displacements, the scratch in the substrate is not continuous because the tip can jump over the surface when slipping, whereas at 15 Å, a continuous scratch is formed. The dynamic friction coefficient increases from ~0.13 to ~0.46 with increasing depth, but the static friction coefficient increases only from ~0.32 to ~0.54. At the larger depths the tip does not come to a halt during stick as it does for shallow indents. Instead the tip motion is more continuous with stick and slip manifested by periods of faster and slower motion. Although the exact points of stick and slip depend on the sliding speed, the damage to the substrate, the atomistic stick-slip mechanisms, and the friction coefficients are relatively independent of speed over the range of values considered.

DOI: 10.1103/PhysRevB.69.205407 PACS number(s): 68.35.Af, 68.35.Gy, 61.72.Bb

I. INTRODUCTION

Stick-slip is a common phenomenon; for example, it is the cause of sound generation (a violin string, a squeaking door, or the chatter of machinery), sensory perception (taste, texture, and feel), earthquakes, granular flow, and so on.[1] In any mechanism where the kinetic friction is less than the static friction there will be a tendency for the motion to be intermittent rather than smooth. The ''stick'' is due to the higher static friction between the surfaces, and the ''slip'' due to the lower kinetic friction during the slip itself.[2] The squeaks and grunts generated by sliding surfaces usually arise from vibrations set up by the intermittent nature of the sliding process itself. Intermittent motion is a common occurrence in sliding mechanisms and a great deal of ingenuity has been used in trying to overcome it, particularly in the operation of automated machinery. Because of the adverse effects of stick-slip, a number of methods are used to prevent it. These methods generally decrease the amplitude of the slip, or the sliding velocity during the slip, either by increased damping, increased inertia, or by increased stiffness of the spring.[3]

Despite the phenomenon of stick-slip occurring over any length scale[4] its origins are still not well understood. In macroscopic situations, Bowden and Tabor[2] attributed elastic deformation as a primary cause of stick-slip but it is not clear that this will also be the case for microscale or nanoscale processes. Atomic scale stick slip in a scanning force microscope (SFM) was first reported by Mate *et al.*[5] Stick slip in a SFM can occur because the tip has to climb the potential hill of the surface atoms and thus is dependent on the direction in which the tip moves. A zig-zag motion of the SFM tip over the surface can occur and for small sliding velocities a distortion of the SFM image is observed as the tip tries to keep to the lowest energy path.[6] For sliding friction, there has also been shown to be a linear increase of the frictional force with the log of the sliding speed until a certain speed of around 0.5×10^{-4} ms^{-1} is reached at which point the frictional force remains approximately constant.[7,8] However, the simulations presented here are several orders of magnitude faster and are concerned with ploughing friction and so are not directly comparable.

Because nanoscale stick-slip is an increasingly important phenomenon, a number of theoretical and experimental investigations have been carried out in recent years. Li *et al.*[9] performed molecular dynamics (MD) simulations of sliding friction showing that elastic deformation of the surface layers can also be a main cause of the atomic-scale stick-slip phenomenon. Other atomistic simulation work can be found in Refs. 10,13,14 and experimental work in, for example, Ref. 10–12. A direct comparison between experiment and simulation is still not completely possible because of limitations between experimental time scales and system sizes and what is currently computationally possible with modern computational resources. However, despite differences between the speed of the tip and and the size of the system, the simulations are able to capture many of the features observed experimentally. Many MD studies of the stick-slip have been concerned with the study of sliding friction.[9,13–15] However, scratch testing is an important practical tool for the investigation of surface mechanical properties and in this investigation ploughing rather than sliding friction is considered. The dynamics of the indenter and the substrate, including the behavior of the different forces in action, the coefficient of friction, at particular stick and slip events are studied during scratching of an Ag(010) surface by an atomistically defined diamond tip. The variation of sliding speed and indentation depth and their effects on the occurrence of the stick-slip events are investigated. Analysis of the local geometric configuration and potential energy of atoms underneath the tip is also performed to probe for any generation of subsurface defects.

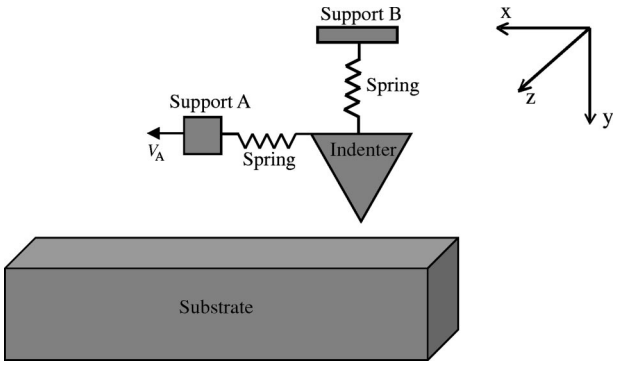

FIG. 1. A schematic diagram of the model used to simulate the stick-slip friction mechanism.

II. METHODOLOGY

Figure 1 shows a diagrammatic representation of the model employed in the MD simulations. The model consists of an indenter attached to two springs, positioned in the horizontal (x) and vertical (y) directions. The supports attached to the springs move with a prescribed velocity. The simulation consists of three stages, namely, the indentation of the substrate, the relaxation of the system, and then scratching of the substrate by the horizontal displacement of the support A.

The indenter is modeled atomistically and is a 90° triangular-based pyramid constructed from a cube corner of a diamond crystal with (100), (010), and (001) faces, so that the normal to the substrate lies in the $\langle 111 \rangle$ direction of the diamond lattice. It is generated with a rounded tip by truncating a number of atoms at the apex.[16–20] The interaction between the indenter atoms is modeled using the Brenner C-C potential.[21,22] The substrate is a face–centered cubic (fcc) silver crystal and is oriented such that the (010) surface is indented. The Ag-Ag interaction is modeled using the Ackland embedded atom method[23] potential and scratching is parallel to the $\langle 100 \rangle$ substrate direction. The interaction between the indenter and the substrate atoms is modeled in a purely repulsive way by the Ziegler-Biersack-Littmack potential.[24] This approach is chosen to simplify the physics since we are interested in investigating the link between material deformation and stick-slip events, rather than adhesion or adsorption. Fixed boundary conditions are applied to the outer two layers of the substrate in the x and z directions. The remaining substrate atoms are damped to remove the surplus of energy added to the system by the indenter. The Lindhard-Scharff inelastic loss model[25] is used for the damping of the atoms so that the temperature of the tip and the substrate does not rise excessively and stabilizes at a low value. This was found to be a reasonable model in previous investigations of nanoindentation.[18] Moreover, all our simulations were started at 0 K.

Simulations were carried out at an indentation depth of 5 Å and at three different sliding speeds of $V_A = 1.0$, 2.5, and 5.0 ms^{-1}, where V_A is the sliding speed of the horizontal support A. Further simulations were performed at indentation depths of 5 and 15 Å and the sliding speed of $V_A = 1.0$ ms^{-1} to study the effect of varying the indentation depth on the stick-slip events. For the simulations performed at indentation depth of 5 Å, the spring constants of the horizontal and vertical springs, used in the calculations were $k_x = 40.05$ Nm^{-1} and $k_y = 240.30$ Nm^{-1}, respectively, whereas for the simulation at the deeper indent of 15 Å, $k_x = 120.15$ Nm^{-1} and $k_y = 352.44$ Nm^{-1}. The mass of the tip was taken to be 3.14×10^{-23} kg. The values of the vertical spring constants were chosen to be consistent with values in an SFM device so that the actual scratch depth was between $\frac{1}{4}$ and $\frac{3}{4}$ the value of the support displacement. For nanoindentation devices the spring constants are typically larger than those used in scanning force microscopy. A value of 352 Nm^{-1} is towards the higher end of those quoted by instrument manufacturers. A similar reasoning was behind the choice of horizontal spring constant, i.e., the spring neither extended excessively during the dynamics nor was so stiff that it behaved as a solid body. If smaller values of the spring constants are used then the spring deforms further before the force builds up sufficiently for the motion to occur. However, too large a value means that there is insufficient flexibility for the spring to extend or compress and the tip motion occurs as a forced motion moving with the prescribed velocity of the support. Some tests were carried out to try to determine a reasonable value for a damping constant for the springs. However, the stick-slip phenomenon was found to be very sensitive to the value of the damping constant with too large a value resulting in a rigid spring with no stick and smaller values giving results which were qualitatively similar to those with no damping. As a result no damping was included in this initial study.

At the beginning of the indentation, the indenter vertex was positioned at a height of 5 Å above the substrate surface, which was outside the cutoff range of the tip-substrate interaction potential. The substrate was then indented to the required indentation depth. Although the support B moves a distance of 5 and 15 Å, the actual indentation depths of the tip apex were 1.25 and 9.86 Å, due to the compression of the apex and the spring during indentation. In the simulations, an indenter of ~4100 atoms is employed, but different substrate sizes are used, depending on the sliding speed and indentation depth in order to increase the efficiency in use of computing resources. The number of substrate atoms and the dimensions of the substrate that are employed in the different simulations are given in Table I.

In performing the simulations, the springs are assumed to be connected to the top $\{111\}$ plane of tip atoms. These atoms are treated as a point mass that move together and experience an integrated vertical force F_y from all the free atoms in the indenter below and also a force from the attached spring. During the indentation phase the fixed atoms are constrained in the horizontal direction. The equation of motion of this point mass is therefore,

$$m a_y(t) = F_y(t) + k_y[y_B(t) - y(t)], \tag{1}$$

where $a_y(t)$ is the vertical acceleration of the indenter atoms at time t, m is the mass of the tip, and $y(t)$ is the vertical displacement. The term $k_y[y_B(t) - y(t)]$ is the spring force on the indenter. The displacement of the vertical support B shown in Fig. 1 is given by $y_B(t) = V_B t$, $0 \leqslant t \leqslant T_I$ and

TABLE I. Table showing the substrate sizes employed in the different MD simulations.

Indentation depth (Å)	Sliding speed of horizontal support (ms^{-1})	Total simulation time (ns)	Dimensions of substrate	Number of substrate atoms
5	1.0	5.0	140 Å×20 Å×80 Å	17 656
5	2.5	4.0	180 Å×20 Å×80 Å	21 656
5	5.0	2.0	180 Å×20 Å×80 Å	21 656
15	1.0	5.0	180 Å×45 Å×100 Å	50 520

$y_B(t)=y_{max}=V_B T_I$, $T_I<t\leqslant T_{rel}$. Here T_I is the indentation time and T_{rel} the time at which the relaxation process ends. In all cases $T_{rel}-T_I$ was fixed at 10 ps.

During scratching, the fixed layer of indenter atoms are displaced in the horizontal direction x by motion of the support A but are constrained in the z direction. The support A is set in motion with a constant speed V_A in the x direction for $t>T_{rel}$ and thus the equations of motion are given as

$$ma_x(t)=F_x(t)+k_x[V_A t-x(t)] \tag{2}$$

and

$$ma_y(t)=F_y(t)+k_y[y_{max}-y(t)], \tag{3}$$

where $a_x(t)$ is the horizontal acceleration of the indenter atoms, $x(t)$ is the horizontal displacement. The force $F_x(t)$ is the integrated force arising from the action of the free indenter atoms with the fixed atoms and is thus also the same as the frictional force arising from the interaction of the tip with the substrate. Since F_x and F_y are time dependent, the friction coefficient $\mu=|F_x/F_y|$ will also be a function of time t. In the presentation of the results that follow, we define the dynamic friction coefficient as the time average value of $\mu(t)$. The static friction coefficient is calculated as the average of the largest maxima of $\mu(t)$.

III. RESULTS AND DISCUSSION

The results will be presented, by making first a comparison between the simulations performed at a fixed vertical support translation of 5 Å but at the three different sliding speeds of $V_A=1.0$, 2.5, and 5.0 ms^{-1}; second, by comparing the results from simulations with the sliding speed of $V_A=1.0$ ms^{-1} but with different indentation depths of 5 Å and 15 Å. Because the tip is modeled atomistically there is some distortion of the tip during both the indentation and the scratching process. For the nominal 5 Å indentation depth, the tip compresses by around 9% (2.4 Å in a tip height of 26.5 Å), which together with the spring compression gives an actual indentation depth of around 1.25 Å. During indentation the tip also undergoes a lateral distortion of 0.6 Å so that the vertex does not lie directly below the center of mass of the top layer as it does at the start of the simulation. The distortion oscillates during the lateral motion, depending on the stick or slip event reaching a maximum of about 1.4 Å corresponding to a twist of $\approx 3°$.

Figures 2(a)–2(c) show the relationship between the horizontal spring force and horizontal displacement, for the three different sliding speeds of the support A. The spring force lies in the approximate range of 0–12 nN, for all the three cases. All the graphs have large maxima located at distances associated with the positions of atomic rows and corresponding to stick events. However, not all atomic rows correspond to such an event showing that slipping over the atomic rows occurs which depends on the sliding speed. Microslip events can be seen at the beginning of the scratching simulations for the cases of $V_A=2.5$ and 5.0 ms^{-1}, shown in Figs. 2(b) and 2(c). For these cases, at the start of the horizontal motion, there is no true stick and the small maxima in these curves are due to the tip sliding over individual rows of substrate atoms (the Ag lattice constant is 4.09 Å), instead of ploughing through the substrate. There are also shoulders on the right slope of each peak which again correspond to the sliding of the tip over individual atomic rows.

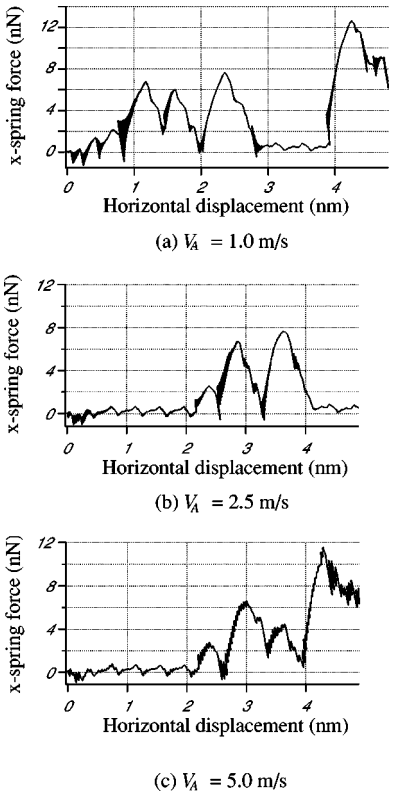

FIG. 2. Figures showing the plot of the horizontal spring force against the horizontal displacement of the indenter, for three different sliding speeds of $V_A=1.0$, 2.5, and 5.0 ms^{-1} at an indentation depth of 5 Å.

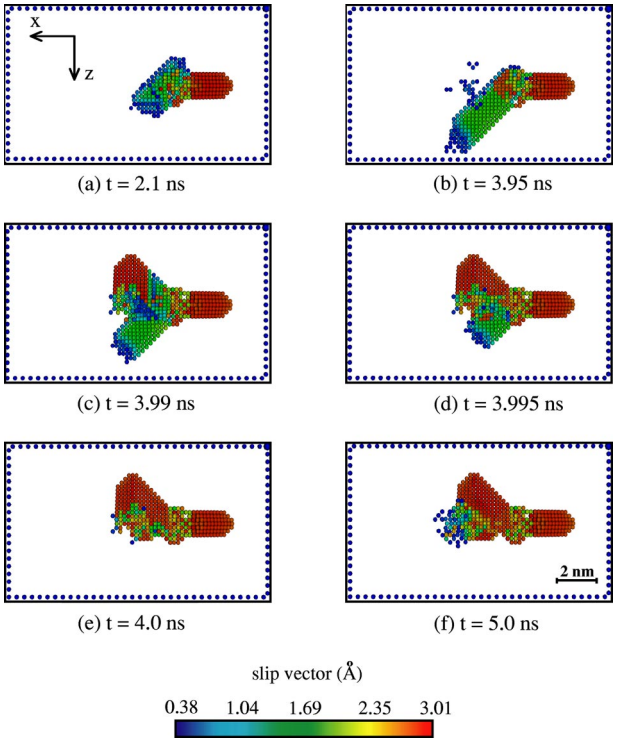

FIG. 3. Figures showing the emission of dislocations for the shallow indent of 5 Å and for a sliding speed of 1.0 ms^{-1}. The figures are colored according to the modulus of the slip vector given in the key.

The motion occurring after a major stick event was found to be associated with plastic deformation of the substrate with the emission of a dislocation in the region below the indenter. This is illustrated in Figs. 3(a)–3(f). Here, the atoms are represented as circles, shaded according to the modulus of the slip vector.[26] The red atoms show the region of the lattice that have undergone a perfect dislocation, with Burgers' vector $\mathbf{b}=\frac{1}{2}\langle 110\rangle$. The green circles represent atoms on a stacking fault. The emission of the dislocations occurs over a short time scale. At the end of the stick process shown in Fig. 3(b), a partial dislocation is emitted in the $\langle 101\rangle$ direction followed by its retraction, Figs. 3(c)–3(e), and the emission of a full dislocation in the $\langle 10\bar{1}\rangle$ direction. This then remains during the rest of the simulation. Figures 3(b)–3(f) should also be compared with Fig. 4(a)–4(c). The stick event is clearly shown in Fig. 4(a) after 4.0 ns when the support and tip motion separates. There is even some motion of the indenter in the reverse horizontal direction until a catching up process occurs. The length of time of the stick event is quite short, of the order of 150 ps. During this time, Fig. 4(c) shows that there is an upward jump of the tip of about 0.5 Å as the stress in the substrate is relieved and the motion begins again. The horizontal spring force also begins to increase during the stick event. The emission of dislocations in the substrate was not observed for a 5 Å depth when the tip was constrained to move with a constant velocity.[20] In that case only elastic deformation of the substrate took place. Here there is plastic deformation when the actual indentation depth is only 1.25 Å. Figure 4(b) plots the velocity of the tip

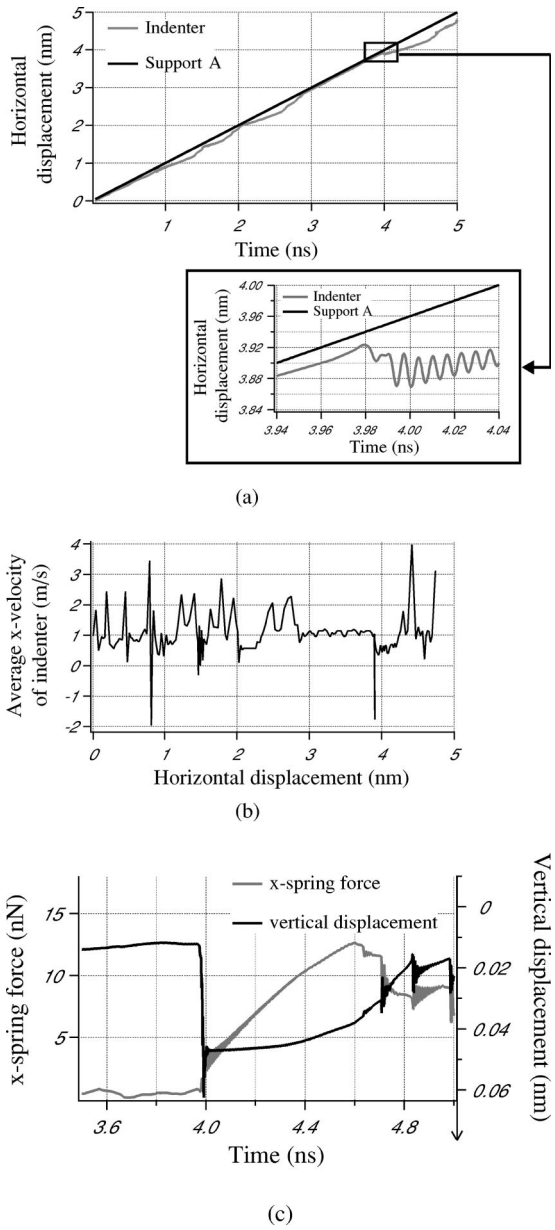

FIG. 4. Figure showing the plot of the (a) horizontal displacement of the indenter and the horizontal support as a function of elapsed time. The points where the tip and the support are farthest separated also correspond to the maximum horizontal distortion of the tip, e.g., 1.4 Å at 4.5 ps; (b) velocity of the indenter in the horizontal direction against the horizontal displacement of the indenter, for the case when the simulation was performed at a sliding speed of $V_A=1.0$ ms^{-1} and at an indentation depth of 5 Å. The velocity is averaged over a time scale of 25 ps; (c) plots of the spring force in the horizontal direction and the vertical displacement of the fixed atoms of the indenter, against time at a sliding speed of 1.0 ms^{-1} and at an indentation depth of 5 Å. Here the zero point for the vertical displacement is after the indentation and relaxation phase.

averaged over 25 ps time windows. There are a number of minima where the tip velocity is zero and even negative, corresponding to stick events and a clear slip event for the horizontal displacement of between 3 and 4 nm.

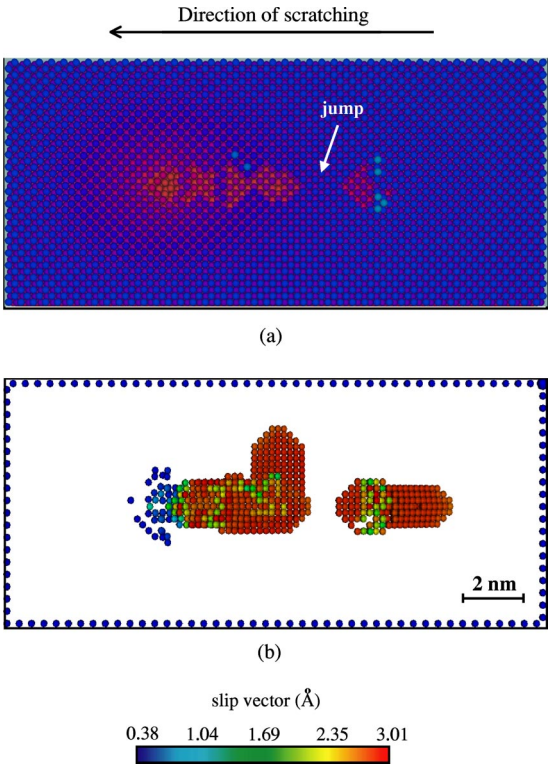

FIG. 5. Figure showing the top view of substrate at the end of the scratching simulation, at the indentation depth of 5 Å and a sliding speed of 2.5 ms^{-1}. (a) is colored by depth, with light blue atoms above the surface and red atoms below the surface; (b) is colored according to the modulus of the slip vector given in the key.

Figure 5(a) shows the top view of the substrate surface at the end of the simulation showing the damage done to the surface by the indenter for a sliding speed of $V_A = 2.5$ ms^{-1}. Figure 5(b) shows the atoms underneath the substrate surface that have moved. The scratch shown in Fig. 5(a), is not continuous compared to that seen in Ref. 20 where the top layer of the tip atoms were constrained to move in a predetermined way without attached springs, because of the slip experienced by the indenter. It can be clearly seen that the initial motion occurs with such a slip event which is marked on the figure. This initial slip occurs also at a speed of 5.0 ms^{-1}. The jump over the surface corresponds exactly to the microslip events already discussed in the horizontal spring force plots of Fig. 2(b). A comparison

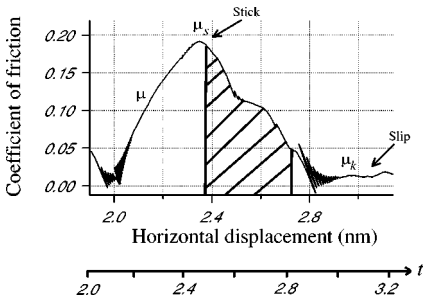

FIG. 6. Plot of the friction coefficient against the horizontal displacement of the indenter, for the case when the simulation was performed at a sliding speed of $V_A = 1.0$ ms^{-1} and at an indentation depth of 5 Å in the domain $t = 2.0$ to $t = 3.2$ ns. μ increases to μ_s to build up tension on the horizontal spring during the stick phase. The indenter slips and the kinetic component μ_k persists.

between the surface damage of the substrate for the three cases where the simulations were performed at sliding speeds of $V_A = 1.0$, 2.5, and 5.0 ms^{-1} shows that the surface damage is qualitatively the same in all three cases except for this initial slip which is more pronounced at the faster speeds. During this slip, of the tip over the surface, Fig. 5(b) shows that no subsurface dislocations form. Dislocations are only formed in the substrate when stress is released after the next stick event. Figure 5(a) shows also that there are few piled up atoms on the surface despite the displacement of surface atoms to form the scratch. These atoms are displaced into the bulk through the dislocation emission process. There is a corresponding but small surface deformation.

The simulations show that the horizontal and vertical forces on the tip are highly correlated. As a result the graphs of the friction coefficient as a function of horizontal distance have almost exactly the same shape as the horizontal force curve given in Fig. 2. Figure 6 shows the variation of the coefficient of friction with horizontal displacement at a sliding speed of $V_A = 1.0$ ms^{-1} and a vertical support displacement of 5 Å, which should be compared with the corresponding curve in Fig. 2(a). Slip is easily recognized not only from the velocity curves but also as corresponding to that part of the curve in Fig. 6 where the friction coefficient has a low value.

Figure 6 shows that there is a stick event at approximately 2.4 nm where the value of μ rises to the maximum value of the static coefficient of friction μ_s. The actual values of

TABLE II. Results of MD simulations for the three different sliding speeds and at the two different indentation depths.

Sliding speed (ms^{-1})	Normal force (nN)	Frictional force (nN)	Dynamic coefficient of friction	Static coefficient of friction
		Indentation depth of 5 Å		
1.0	28.3	3.8	0.13	0.32
2.5	28.3	2.6	0.09	0.28
5.0	28.0	2.8	0.10	0.29
		Indentation depth of 15 Å		
1.0	106.1	49.1	0.46	0.54

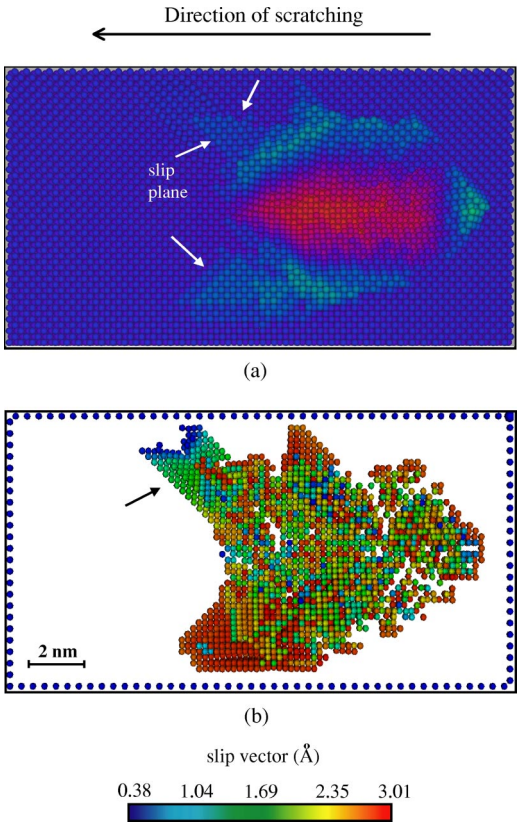

FIG. 7. Figures showing the top view of substrate at the end of the scratching simulation, at an indentation depth of 15 Å and a sliding speed of 1.0 ms^{-1}. (a) is colored on depth, where the light blue-colored spheres around the edge of the hole represent piled up atoms on the surface and red spheres represent subsurface atoms; (b) is colored according to the modulus of the slip vector. The slip planes on the substrate surface are marked by the white arrows in (a). The black arrow in (b) shows the dislocation underneath the scratch groove, which corresponds to the slip plane in (a).

static friction coefficient μ_s given in Table II are an average of the largest peaks of the friction coefficient over the length of the scratch. The average normal and horizontal frictional forces and hence the dynamic friction coefficients for the three different sliding speeds and the two different indentation depths are also calculated and the values are given in Table II. Comparing the values of the static and dynamic friction coefficients at the indentation depth of 5 Å for the three different sliding speeds we can see that μ_s takes a value of around 0.3, whereas the dynamic friction coefficient takes a value of around 0.1. However, the dynamic friction coefficient at an indentation depth of 15 Å increases almost three times compared to the value obtained from the simulation performed at 5 Å. The static friction coefficient increases slightly less from 0.3 to 0.5. The value of the dynamic friction coefficient of 0.46 for the vertical support displacement of 15 Å, corresponding to an actual tip depth of 9.86 Å, agrees almost exactly with the value of 0.41 previously calculated for an indenter constrained to move with a fixed speed at a depth of 10 Å.[20]

Figure 7(a) shows the surface damage for the simulation performed at indentation depth of 15 Å and at sliding speed

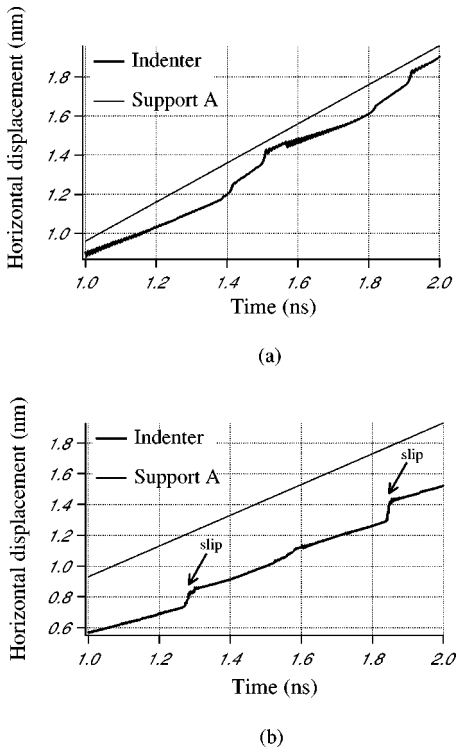

FIG. 8. Graphs showing the horizontal displacement of the indenter and the horizontal support A at a sliding speed of $V_A = 1.0$ ms^{-1} and indentation depths of (a) 5 Å and (b) 15 Å.

of 1.0 ms^{-1}. Here the maximum height of the pileup of silver atoms is ~7.9 Å compared to the case of the shallow indent, where just a few adatoms were observed. The pileup can also explain the higher static and dynamic friction coefficients for the case of the deeper indent, shown in Table II, since the piled up material itself also acts as a resistance to the motion. This link between the pileup and the friction coefficient was also observed in Ref. 20. Figure 7(a) also shows a continuous scratch with no slipping over the surface at this depth and Fig. 7(b) shows the corresponding subsurface damage, which is also more evenly distributed than that for the shallower indent. At a particular slip event the indenter still displaces slightly in the negative y direction but because the depth is greater, ~9.9 Å, it continues to plough through the substrate instead of sliding over the surface as observed for the case of the shallow indent. Figures 8(a) and 8(b) show the horizontal displacement of the indenter and the support A for the simulations at a sliding speed of 1.0 ms^{-1} and indentation depths of 5 and 15 Å, respectively. For the 15 Å curve in Fig. 8(b), slip events can be observed where the horizontal displacement increases sharply but sticking occurs not by the tip coming to an actual halt as it did at 5 Å and 4 ns in Fig. 4(a) but by a slow tip speed which is less than that of the support as seen by the smaller gradient of the indenter curve compared to the support curve.

Figures 9(a) and 9(b) compare the horizontal spring forces for the two scratching depths. The maxima in Fig. 9(a) corresponds to the positions of atomic rows of atoms. The spring force is approximately ten times higher for indentation depth of 15 Å, Fig. 9(b), compared to that at 5 Å, Fig.

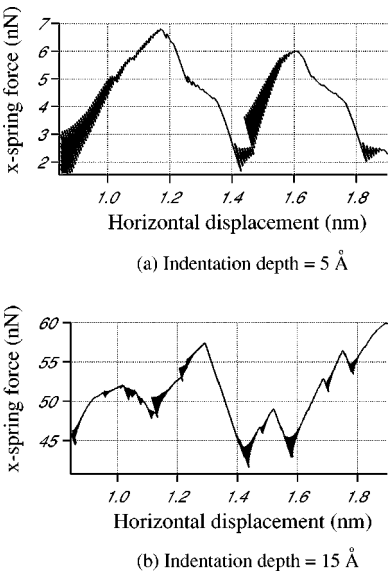

FIG. 9. Graphs showing the plot of the horizontal spring force against horizontal displacement of the indenter at a sliding speed of 1.0 ms^{-1} and indentation depths of (a) 5 Å and (b) 15 Å, in the range of $t=1.0$ to $t=2.0$ ns.

9(a), and at the deeper depths there is no correspondence between the horizontal spring force maxima and the positions of atomic rows.

IV. CONCLUSION

A model is developed to investigate the atomic-scale stick-slip phenomenon for a pyramidal diamond tip in contact with the (010) surface of fcc silver. The MD simulations illustrate some important mechanisms that take place during stick slip in this system. In particular they show that stick slip is associated with the production of dislocations in the substrate below the indenter. Such dislocations were not observed at an equivalent indentation depth when dragging the tip at a constant speed and fixed depth.[20]

Varying the support sliding speed does have an effect on the motion of the tip. At faster speeds the initial impulse to the motion is transmitted through the spring causing an initial slip event which does not occur at the lower speeds. Increasing the depth of the indenter gives a continuous line of damage to the substrate, and then stick slip is manifested by periods of motion where the tip moves faster and then slower than the support (but does not come to a halt) and by the partly irregular shape of sides and bottom of the scratch.

The dynamic coefficient of friction, which is an average value over the length of the scratch, calculated using the spring model is almost identical to that previously calculated with the forced motion model, indicating that average frictional forces during the stick and slip events, where these forces are both high and low in turn, are similar to that for continuous motion. However, the stick-slip model allows the calculation of the static friction coefficient which was not possible previously. These static values are about three times larger than the dynamic values at a depth of 5 Å but lie closer to the dynamic values at 15 Å, as might be expected because of the more uniform motion at the deeper ploughing depths.

The success of the spring model in capturing the essential features of the stick-slip process during shallow surface scratching gives us confidence to investigate more complex systems where the effect of other parameters such as temperature and adhesion between surfaces can be fully explored.

ACKNOWLEDGMENTS

This work has been funded by the EPSRC, Grants No. GR/R18581/01 and GR/R67699/02. One of the authors (D.M.) would like to thank the EPSRC and Loughborough University for support. We would also like to thank Asta Richter of the University of Applied Sciences, Wildau, and Bruce King of the University of Newcastle, Australia for useful discussions. The calculations were carried out using Loughborough University's high performance computing and visualization facility.

[1] B. Bhushan, *Modern Tribology Handbook 1* (CRC Press, Boca Raton, FL, 2001).
[2] F.P. Bowden and D. Tabor, *The Friction and Lubrication of Solids* (Clarendon, Oxford, 1954).
[3] E. Rabinowicz, *Friction and Wear of Materials* (Wiley, New York, 1965).
[4] A.L. Demirel and S. Granick, Phys. Rev. Lett. **77**, 4330 (1996).
[5] C.M. Mate, G.M. McClelland, R. Erlandsson, and S. Chiang Phys. Rev. Lett. **59**, 1942 (1987).
[6] U.D. Schwarz, O. Zwörner, P. Köster, and R. Wiesendanger, Phys. Rev. B **56**, 6987 (1997).
[7] E. Riedo, E. Gnecco, R. Bennewitz, E. Meyer, and H. Brune, Phys. Rev. Lett. **91**, 084502 (2003).
[8] Y. Sang, M. Dubé, and M. Grant, Phys. Rev. Lett. **87**, 174301 (2001).
[9] Bin Li, P.C. Clapp, J.A. Rifkin, and X.M. Zhang, J. Appl. Phys. **90**, 3090 (2001).
[10] T. Cagin, J. Che, M.N. Gardos, and A. Fijany, Nanotechnology **10**, 278 (1999).
[11] M. Brandbyge, J. Schiøtz, M.R. Sørensen, P. Stoltze, K.W. Jacobsen, J.K. Nørskov, L. Olesen, E. Laegsgaard, I. Stensgaard, and F. Besenbacher, Phys. Rev. B **52**, 8499 (1995).
[12] S. Fujisawa, E. Kishi, Y. Sugawara, and S. Morita, Phys. Rev. B **51**, 7849 (1995).
[13] M.R. Sørensen, K.W. Jacobsen, and P. Stoltze, Phys. Rev. B **53**, 2101 (1996).
[14] J.A. Harrison, C.T. White, R.J. Colton, and D.W. Brenner, Phys. Rev. B **46**, 9700 (1992).
[15] J. Shimizu, H. Eda, M. Yoritsune, and E. Ohmura, Nanotechnology **9**, 118 (1998).
[16] D. Christopher, R. Smith, and A. Richter Nucl. Instrum. Methods Phys. Res. B **180**, 117 (2001).

[17] D. Christopher, R. Smith, and A. Richter, Nanotechnology **12**, 372 (2001).
[18] R. Smith, D. Christopher, S.D. Kenny, A. Richter, and B. Wolf Phys. Rev. B **67**, 245405 (2003).
[19] D. Mulliah, D. Christopher, S.D. Kenny, and R. Smith, Nucl. Instrum. Methods Phys. Res. B **202**, 294 (2003).
[20] D. Mulliah, S.D. Kenny, R. Smith, and C.F. Sanz-Navarro, Nanotechnology **15**, 2243 (2004).
[21] D.W. Brenner, Phys. Rev. B **42**, 9458 (1990).
[22] D.W. Brenner, Phys. Rev. B **46**, 1948 (1992).
[23] G.J. Ackland, G. Titchy, V. Vitek, and M.W. Finnis, Philos. Mag. A **56**, 735 (1987).
[24] J.P. Biersack, J. Ziegler, and U. Littmack, *The Stopping and Range of Ions in Solids* (Pergamon, Oxford, 1985).
[25] J. Lindhard, M. Scharff, and H.E. Schiott, K. Dan. Vidensk. Selsk. Mat. Fys. Medd. **33**, 14 (1963).
[26] O. Rodríguez de la Fuente, J.A. Zimmerman, M.A. González, de la J. Figuera, J.C. Hamilton, Pai Woei Wu, and J.M. Rojo, Phys. Rev. Lett. **88**, 036101 (2002).